Charge symmetry violation in the structure of the ^{3}H-^{3}He system

S. Barshay*
III. Physikalisches Institut, Technische Hochschule, Aachen, Federal Republic of Germany and Research Institute for Fundamental Physics, Kyoto, Japan

L. M. Sehgal
III. Physikalisches Institut, Technische Hochschule, Aachen, Federal Republic of Germany
(Received 20 February 1985)

A geometrical model is proposed for the distribution of matter in the ^{3}H-^{3}He system, incorporating a short-range three-nucleon correlation. Charge symmetry violation is introduced through a distortion of this correlation in going from ^{3}H to ^{3}He. The model is able to describe the charge-symmetry violating effects observed in $\pi^{\pm}$ scattering from these nuclei. When adjusted to fit the high q^2 behavior of the ^{3}He charge form factor, the model yields a prediction for the corresponding structure in ^{3}H.

I. INTRODUCTION

Evidence of charge symmetry violation has been reported in a recent experiment[1] that has studied $\pi^{\pm}$ scattering from the three-nucleon systems ^{3}H and ^{3}He. The experiment, performed at the first pion-nucleon resonance with $\pi^{\pm}$ of kinetic energy 180 MeV, measures the ratios of differential cross sections

$$r_1=\frac{d\sigma(\pi^+ + {}^3\mathrm{H})}{d\sigma(\pi^- + {}^3\mathrm{He})}\,,\quad r_2=\frac{d\sigma(\pi^- + {}^3\mathrm{H})}{d\sigma(\pi^+ + {}^3\mathrm{He})} \tag{1a}$$

at scattering angles from 40° to 90°. The "super-ratio"

$$R=r_1 r_2\,, \tag{1b}$$

in particular, is stated to be free of all systematic errors in its *variation* with θ. The ratios r_1, r_2, and R would be equal to one at all angles if charge symmetry invariance were exact. The experimental results, shown in Figs. 1(a)–(c), indicate a violation of charge symmetry with several striking features, namely (i) the size of the effect: $R=1.31\pm0.09$ at its maximum; (ii) the angular variation of $R(r_2)$, in particular the sharp fall from its maximum to nearly unity at 90°; and (iii) the difference in behavior of r_1 and r_2.

An immediate question is whether the effects observed are attributable to the charge-dependent Coulomb force acting between the $\pi^{\pm}$ and the nuclei ^{3}H and ^{3}He. The authors of Ref. 1 have examined several sources of such "trivial" charge symmetry violation. The pure Coulomb interaction $d\sigma_C=|A_C|^2$ is estimated to give an effect of about 1% at the scattering angles relevant to the experiment. The Coulomb-nuclear interference term $2A_CA_N\cos\phi$ is small since the relative phase ϕ is near 90° for $T_\pi=180$ MeV. Even for an arbitrary phase, the maximum effect is $<5\%$ in r_1 and r_2 and cancels to first order in R. The Coulomb energy shift is estimated to increase r_1 by 3% and decrease r_2 by a similar amount. The Coulomb distortion of the pion-nucleus potential is estimated to be small and of the wrong sign to explain the measured ratios. Altogether such Coulomb effects are claimed to be less than 7%, too small to account for the observations in Fig. 1.

In this paper, we accept the data and the above arguments at face value and seek an explanation of the charge

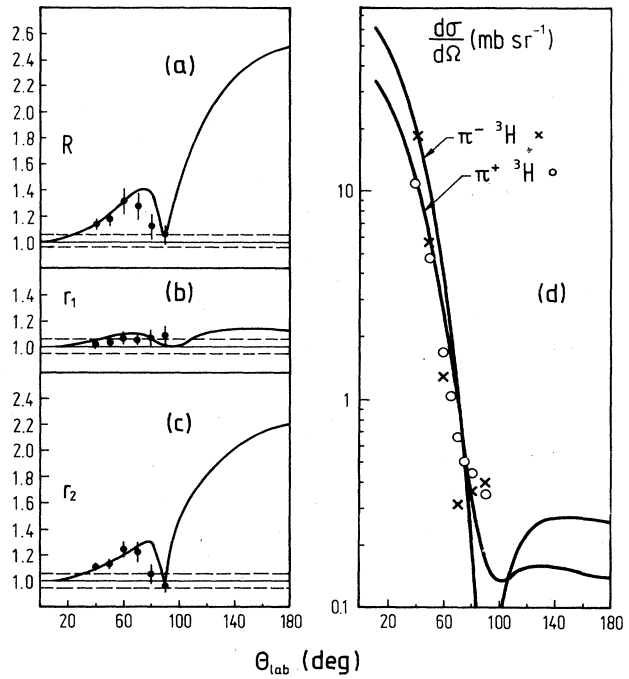

FIG. 1. (a) The product of the differential cross section ratios $r_1r_2=R=d\sigma(\pi^+{}^3\mathrm{H})d\sigma(\pi^-{}^3\mathrm{H})/d\sigma(\pi^-{}^3\mathrm{He})d\sigma(\pi^+{}^3\mathrm{He})$. (b) The ratio $r_1=d\sigma(\pi^+{}^3\mathrm{H})/d\sigma(\pi^-{}^3\mathrm{He})$. (c) The ratio $r_2=d\sigma(\pi^-{}^3\mathrm{H})/d\sigma(\pi^+{}^3\mathrm{He})$. (d) Differential cross sections $d\sigma(\pi^{\pm}{}^3\mathrm{H})$. The data, with systematic error shown as dashed lines, are from Ref. 1 at pion kinetic energy of 180 MeV. The theoretical curves are from Eqs. (11). In (d), $d\sigma(\pi^-{}^3\mathrm{H})$ is normalized to the data point at 40°.

symmetry violating effects in terms of the structure of the ^{3}H and ^{3}He nuclei. A simple geometrical model is proposed that accounts for the observations in Fig. 1. The specific geometrical feature is a three-nucleon correlation that is assumed to arrange the nucleons in a triangular configuration. The observed charge symmetry violation arises in part from the Coulomb distortion of this triangle in going from ^{3}H to ^{3}He. A three-nucleon correlation of this type could conceivably arise from an underlying dynamics that includes three-body forces. [It may be recalled that standard two-body forces are unable to reproduce the binding energies of ^{3}H and ^{3}He (Ref. 2), and that explicit inclusion of three-body forces appears to improve the situation.[3]] The model presented below is, however, purely geometrical and no connection with dynamics is attempted at this stage.

A three-nucleon triangular configuration has also been invoked[4] in the past to understand another peculiar feature of the ^{3}He system, namely its charge form factor as measured by electron scattering at large momentum transfers,[5] which suggests the existence of a "hole" or depression in the central charge density of this nucleus. Such a hole is readily associated with the deficit of matter at the body center of a triangular correlation. By adjusting our model to reproduce the structure observed in the charge form factor of ^{3}He, we are able to generate a prediction for the corresponding structure in ^{3}H, which can be tested by experiments that are now in progress.

II. DESCRIPTION OF THE MODEL

In the limit of charge symmetry, the ^{3}H-^{3}He system forms an isotopic doublet, and the proton and neutron distributions in these nuclei are described by (matter) form factors which are related by

$$F^{^3\mathrm{H}}_{\mathrm{p,n}}(q^2)=F^{^3\mathrm{He}}_{\mathrm{n,p}}(q^2) \quad \text{(charge symmetry)} . \tag{2}$$

This relationship is destroyed by the repulsive Coulomb force between the two protons in ^{3}He. Our objective is to make a geometrical model for this Coulomb-induced distortion and trace its consequences.

Consider first the triton nucleus ^{3}H which is undisturbed by Coulomb forces. We assume, for simplicity, a common distribution for the proton and neutrons in this nucleus. (Possible deviations from this assumption will be commented upon in Sec. V.) Our basic ansatz is that the distribution of nucleons in ^{3}H may be represented by a form factor

$$F^{^3\mathrm{H}}_{\mathrm{p,n}}(q^2)=(1-\epsilon)e^{-R_1^2q^2/6}+\epsilon e^{-\eta^2R_{\mathrm{N}}^2q^2} , \tag{3}$$

which is a superposition of two distributions which we (initially) approximate by Gaussians. The first piece, with probability $(1-\epsilon)$, represents independent particle motion of the three nucleons within a volume of radius R_1 (which we anticipate to be of order 1.6–1.7 fm). The second piece with weight ϵ represents a Gaussian approximation to a short-range three-nucleon correlation of the type depicted in Fig. 2(a), which shows the nucleons in a close-packing equilateral configuration. The size of this correlation is determined by the constant η which is treated as an adjustable parameter. The nucleon radius $R_{\mathrm{N}}=0.8$ fm is introduced as a scale.

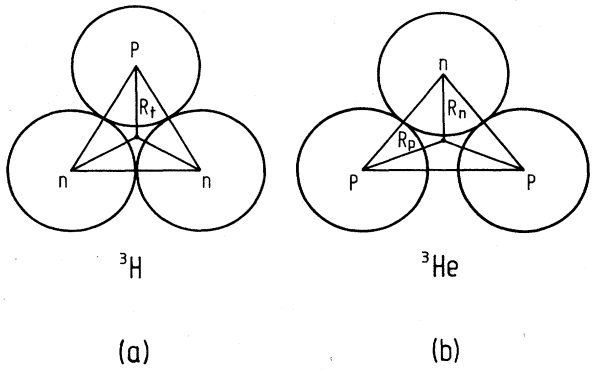

FIG. 2. Three-nucleon triangular configurations in ^{3}H and ^{3}He.

In going from ^{3}H to ^{3}He, the Coulomb repulsion of the two protons induces a violation of charge symmetry, i.e.,

$$F^{^3\mathrm{H}}_{\mathrm{p,n}}(q^2)\neq F^{^3\mathrm{He}}_{\mathrm{n,p}}(q^2) \quad \text{(charge symmetry violation)} . \tag{4}$$

This violation occurs in two ways: (i) the independent particle motion of the three nucleons in ^{3}He is characterized by a slightly expanded radius $R_2>R_1$; (ii) the short range piece of the form factor in ^{3}He is characterized by a distorted triangle [Fig. 2(b)], the Coulomb repulsion of the protons converting the equilateral configuration of ^{3}H into an isosceles configuration. In consequence, the proton and neutron distributions in ^{3}He are described by matter form factors parametrized as

$$F^{^3\mathrm{He}}_{\mathrm{p,n}}(q^2)=(1-\epsilon)e^{-R_2^2q^2/6}+\epsilon e^{-\eta_{\mathrm{p,n}}^2R_{\mathrm{N}}^2q^2} . \tag{5}$$

The geometry of the triangles shown in Fig. 2 yields a relation between η, η_{p}, and η_{n} (note that $R_t:R_{\mathrm{p}}:R_{\mathrm{n}}=\eta:\eta_{\mathrm{p}}:\eta_{\mathrm{n}}$):

$$\eta_{\mathrm{p}}^2+2\eta_{\mathrm{n}}^2=3\eta^2 . \tag{6}$$

This relation is the essential feature we abstract from the triangle correlation. The resulting hierarchy $\eta_{\mathrm{p}}>\eta>\eta_{\mathrm{n}}$ implies a specific pattern to the charge symmetry violation in the short-range part of the ^{3}H and ^{3}He form factors. In particular, when q^2 is large enough that the pieces proportional to ϵ are dominant, the model predicts

$$F^{^3\mathrm{He}}_{\mathrm{n}}>F^{^3\mathrm{H}}_{\mathrm{p,n}}>F^{^3\mathrm{He}}_{\mathrm{p}} . \tag{7}$$

In the next section we shall find that the charge-symmetry violating effects observed in $\pi^{\pm}$ scattering (Fig. 1) can be understood in terms of such a hierarchy.

III. APPLICATION TO $\pi^{\pm}$ SCATTERING

We consider $\pi^{\pm}$ scattering from ^{3}H and ^{3}He, treating these as static distributions of nucleons described by the form factors given in Eqs. (3) and (5). Since these nuclei have spin $\frac{1}{2}$, the differential cross section is

$$\frac{d\sigma}{d\Omega}=|f|^2+|g|^2 , \tag{8}$$

where f and g denote the spin-nonflip and spin-flip amplitudes, respectively. At a kinetic energy of 180 MeV, the incident pion scatters from individual static nucleons in a resonant P wave, with total angular momentum $J=\frac{3}{2}$ and total isospin $T=\frac{3}{2}$. The pion-nucleon amplitudes, up to a phase factor i, are

$$\begin{aligned} &f(\pi^+\mathrm{p})=f(\pi^-\mathrm{n})=2\cos\theta, \quad f(\pi^+\mathrm{n})=f(\pi^-\mathrm{p}) \\ &\qquad =\tfrac{2}{3}\cos\theta , \\ &g(\pi^+\mathrm{p})=g(\pi^-\mathrm{n})=\sin\theta, \quad g(\pi^+\mathrm{n})=g(\pi^-\mathrm{p}) \\ &\qquad =\tfrac{1}{3}\sin\theta , \end{aligned} \tag{9}$$

so that the corresponding amplitudes for scattering on the $A=3$ nuclei are

$$\begin{aligned} f(\pi^{+3}\mathrm{H})&=2\cos\theta F_{\mathrm{p}}^{^3\mathrm{H}}+\tfrac{4}{3}\cos\theta F_{\mathrm{n}}^{^3\mathrm{H}} , \\ f(\pi^{-3}\mathrm{H})&=\tfrac{2}{3}\cos\theta F_{\mathrm{p}}^{^3\mathrm{H}}+4\cos\theta F_{\mathrm{n}}^{^3\mathrm{H}} , \\ g(\pi^{+3}\mathrm{H})&=\sin\theta F_{\mathrm{p}}^{^3\mathrm{H}} , \\ g(\pi^{-3}\mathrm{H})&=\tfrac{1}{3}\sin\theta F_{\mathrm{p}}^{^3\mathrm{H}} , \\ f(\pi^{+3}\mathrm{He})&=4\cos\theta F_{\mathrm{p}}^{^3\mathrm{He}}+\tfrac{2}{3}\cos\theta F_{\mathrm{n}}^{^3\mathrm{He}} , \\ f(\pi^{-3}\mathrm{He})&=\tfrac{4}{3}\cos\theta F_{\mathrm{p}}^{^3\mathrm{He}}+2\cos\theta F_{\mathrm{n}}^{^3\mathrm{He}} , \\ g(\pi^{+3}\mathrm{He})&=\tfrac{1}{3}\sin\theta F_{\mathrm{n}}^{^3\mathrm{He}} , \\ g(\pi^{-3}\mathrm{He})&=\sin\theta F_{\mathrm{n}}^{^3\mathrm{He}} . \end{aligned} \tag{10}$$

In writing Eq. (10), we have assumed that the like nucleons in ^{3}H and ^{3}He maintain their usual coupling to spin zero, so that the spin-flip scattering involves the unlike nucleon only. From Eqs. (8) and (10), we obtain the ratios r_1 and r_2:

$$\begin{aligned} r_1&=\frac{d\sigma(\pi^+ +{}^3\mathrm{H})}{d\sigma(\pi^- +{}^3\mathrm{He})}=\frac{[(\frac{5}{3})^2(4\cos^2\theta)+\sin^2\theta][(1-\epsilon)F_1+\epsilon F_t]^2}{(4\cos^2\theta)[\frac{5}{3}(1-\epsilon)F_2+\epsilon(\frac{2}{3}F_{\mathrm{p}}+F_{\mathrm{n}})]^2+\sin^2\theta[(1-\epsilon)F_2+\epsilon F_{\mathrm{n}}]^2} , \\ r_2&=\frac{d\sigma(\pi^- +{}^3\mathrm{H})}{d\sigma(\pi^+ +{}^3\mathrm{He})}=\frac{[(\frac{7}{3})^2(4\cos^2\theta)+\frac{1}{9}\sin^2\theta][(1-\epsilon)F_1+\epsilon F_t]^2}{(4\cos^2\theta)[\frac{7}{3}(1-\epsilon)F_2+\epsilon(2F_{\mathrm{p}}+\frac{1}{3}F_{\mathrm{n}})]^2+\frac{1}{9}\sin^2\theta[(1-\epsilon)F_2+\epsilon F_{\mathrm{n}}]^2} , \end{aligned} \tag{11}$$

where we have used the abbreviations

$$F_t\equiv e^{-\eta^2 R_{\mathrm{N}}^2 q^2}, \quad F_{\mathrm{p,n}}\equiv e^{-\eta_{\mathrm{p,n}}^2 R_{\mathrm{N}}^2 q^2}, \quad F_{1,2}\equiv e^{-R_{1,2}^2 q^2/6} . \tag{12}$$

The terms in $4\cos^2\theta$ and $\sin^2\theta$ represent the spin-independent and spin-dependent contributions, respectively; for scattering on a free nucleon, these simply add to give the familiar $(3\cos^2\theta+1)$.

The following general observations may be made: (i) In the limit $F_1=F_2$ and *either* $\epsilon=0$ *or* $F_t=F_{\mathrm{p}}=F_{\mathrm{n}}$, we have $r_1=r_2=1$ at all θ, and so no violation of charge symmetry. (ii) Quite generally, one sees from Eq. (11) that $r_1=r_2=1$ at $\theta=0$, and $r_1=r_2$ at $\theta=\pi/2$, where only the spin-dependent scattering contributes. Within our model, the detailed structure of r_1 and r_2, and the difference in their behavior arise as a combined effect of the slightly larger independent particle radius of ^{3}He ($R_2>R_1$) and the hierarchy $F_{\mathrm{n}}>F_t>F_{\mathrm{p}}$ generated by the distortion of the three-nucleon correlation.

In Fig. 1, we show a fit to the data on $\pi^\pm$ scattering with the following parameters:

$$\begin{aligned} &\epsilon=0.27, \quad R_1=1.67\ \mathrm{fm}, \quad R_2=1.74\ \mathrm{fm} \\ &\eta^2=0.33, \quad \eta_{\mathrm{p}}^2=0.45 . \end{aligned} \tag{13}$$

The remaining parameter η_{n}^2 is determined by Eq. (6) to be 0.27. The parameters of this fit were constrained by demanding that the model simultaneously describe the charge form factors of ^{3}H and ^{3}He over the same domain of low q^2 ($q^2<8\ \mathrm{fm}^{-2}$).[5,6] The charge form factors are defined by

$$\begin{aligned} F_{\mathrm{charge}}^{^3\mathrm{H}}&=F_{\mathrm{p}}^{^3\mathrm{H}}f_{\mathrm{p}}+2F_{\mathrm{n}}^{^3\mathrm{H}}f_{\mathrm{n}} , \\ F_{\mathrm{charge}}^{^3\mathrm{He}}&=F_{\mathrm{p}}^{^3\mathrm{He}}f_{\mathrm{p}}+\tfrac{1}{2}F_{\mathrm{n}}^{^3\mathrm{He}}f_{\mathrm{n}} , \end{aligned} \tag{14}$$

where $f_{\mathrm{p}}(q^2)$ and $f_{\mathrm{n}}(q^2)$ are the charge form factors of the proton and neutron which we take to be[7]

$$\begin{aligned} f_{\mathrm{p}}(q^2)&=\left[1+\frac{q^2}{18}\right]^{-2} , \\ f_{\mathrm{n}}(q^2)&=\left[1+\frac{q^2}{20.7}\right]^{-2}-\left[1+\frac{q^2}{17.4}\right]^{-2} , \end{aligned} \tag{15}$$

where q^2 is measured in fm^{-2}. As seen from the comparison in Table I the parameters chosen to fit the $\pi^\pm$ data provide a simultaneous fit to the charge form factors of ^{3}H and ^{3}He at low q^2. In particular, the charge radii are given by

$$\begin{aligned} \langle R^2\rangle_{\mathrm{charge}}^{^3\mathrm{H}}&=(1-\epsilon)R_1^2+6\epsilon\eta^2R_{\mathrm{N}}^2 \\ &\quad +\langle r^2\rangle_{\mathrm{p}}+2\langle r^2\rangle_{\mathrm{n}}=(1.68\ \mathrm{fm})^2 , \\ \langle R^2\rangle_{\mathrm{charge}}^{^3\mathrm{He}}&=(1-\epsilon)R_2^2+6\epsilon\eta_{\mathrm{p}}^2R_{\mathrm{N}}^2 \\ &\quad +\langle r^2\rangle_{\mathrm{p}}+\tfrac{1}{2}\langle r^2\rangle_{\mathrm{n}}=(1.82\ \mathrm{fm})^2 , \end{aligned} \tag{16}$$

where $\langle r^2\rangle_{\mathrm{p}}\approx 0.7\ \mathrm{fm}^2$ and $\langle r^2\rangle_{\mathrm{n}}\approx -0.12\ \mathrm{fm}^2$ are the

TABLE I. Charge form factors of ^{3}H and ^{3}He at low q^2. Comparison of model with data (Refs. 5 and 6).

	$F^{ch}_{^3H}(q^2)$		$F^{ch}_{^3He}(q^2)$	
q^2 (fm^{-2})	Model	Data (Ref. 6)	Model	Data (Ref. 5)
1	0.631	0.622 (7)	0.583	0.576 (7)
2	0.403	0.387 (7)	0.345	0.339 (4)
3	0.262	0.267 (5)	0.207	0.204 (3)
4	0.173	0.175 (4)	0.126	0.130 (3)
5	0.116	0.118 (4)	0.0772	0.0822 (14)
6	0.0783	0.0758 (41)	0.0475	0.0514 (8)
7	0.0534		0.0290	0.0324 (11)
8	0.0365	0.0295 (39)	0.0172	0.0202 (14)

mean square charge radii of the proton and neutron. The results (16) compare well with the experimentally measured[6] charge radii 1.70 ± 0.05 fm for ^{3}H and 1.87 ± 0.05 fm for ^{3}He.

Referring to Fig. 1 again, it should be stressed that the $\pi^\pm$ results cannot be understood solely by postulating $R_1\neq R_2$ with $\epsilon=0$, since in this case we would have $r_1(\theta)\equiv r_2(\theta)$ rising monotonically to about 1.36 at $\theta=\pi/2$. The model predicts large charge-symmetry violation at backward scattering angles ($\theta>90°$), where the behavior of r_1 and r_2 is also strikingly different. In Fig. 1(d), we show the results for the individual cross sections $d\sigma(\pi^-{}^3\mathrm{H})$ and $d\sigma(\pi^+{}^3\mathrm{H})$. Despite the simplistic character of the model (static nucleons, neglect of multiple scattering, etc.) the model describes correctly the falloff of the data over two orders of magnitude, in particular the crossover of the two cross sections at about 70°. At small angles, the measured $\pi^-{}^3$H cross section is about a factor of 2 larger than $\pi^+{}^3$H, in agreement with the theoretically expected ratio $(\frac{7}{5})^2$.

IV. APPLICATION TO CHARGE FORM FACTORS AT LARGE q^2

We now address the question of the dynamical structure observed[8] in the charge form factor of ^{3}He at large q^2 ($10<q^2<100$ fm^{-2}), shown in Fig. 3(a). The prominent features of $|F^{^3He}_{charge}(q^2)|$ are (i) the minimum at $q^2=11.6$ fm^{-2}, (ii) the high maximum at $q^2=17$ fm^{-2}, and (iii) the subsequent slow falloff, with a second possible minimum at $q^2\gtrsim 65$ fm^2, although here the scarce data (at the level of one event per week at SLAC) do not allow a firm statement. The Fourier transform of this charge form factor produces a spatial nucleon density $\rho(R)$ with the remarkable property of a depression at the center $R=0$.[5]

The short-range triangle configuration we have invoked provides a natural mechanism for such a depression. In our previous discussion, however, the matter form factor associated with this correlation was approximated by a Gaussian. While this is adequate for a discussion of the $\pi^\pm$ scattering data at low q^2 ($q^2<8$ fm^{-2}), we now consider a perturbed form that reproduces the observed behavior of the ^{3}He charge form factor. This is done by adding a correction term to the previous parametrization (3) and (5) in the following manner:

$$F^{^3H}_{p,n}(q^2)=(1-\epsilon)e^{-R_1^2q^2/6}+\epsilon[e^{-\eta^2R_N^2q^2}+\delta F(q^2;\lambda)]\,,$$
$$F^{^3He}_{p}(q^2)=(1-\epsilon)e^{-R_2^2q^2/6}+\epsilon[e^{-\eta_p^2R_N^2q^2}+\delta F(q^2;\lambda\eta_p/\eta)]\,, \tag{17}$$
$$F^{^3He}_{n}(q^2)=(1-\epsilon)e^{-R_2^2q^2/6}+\epsilon[e^{-\eta_n^2R_N^2q^2}+\delta F(q^2;\lambda\eta_n/\eta)]\,.$$

Here we denote generically by λ any parameters with the dimension of length which appear in the correction $\delta F(q^2;\lambda)$ to the triton form factor. The assumption that this correction is associated with the details of the triangle correlation implies that the corresponding corrections $F^{^3He}_{p,n}$ are obtained by rescaling $\lambda\to\lambda\eta_{p,n}/\eta$. The geometrical relationship (6) then gives a definite relationship between the high q^2 behavior of the matter form factors $F^{^3H}_{p,n}$ and $F^{^3He}_{p,n}$. The correction terms δF must, of course, be zero at $q^2=0$. In the Appendix, we give an explicit parametrization of δF which is constructed so as to vanish strongly at $q^2=0$, thus ensuring that the parameters of the low q^2 fit (13) are left essentially unaltered.

In Fig. 3(a) we show a fit to the charge form factor $F^{^3He}_{charge}(q^2)$ using the matter form factors (17) and the formulas (14) and (15). The fit reproduces the dip at $q^2=11.6$ fm^{-2}, the secondary maximum at $q^2=17$ fm^{-2},

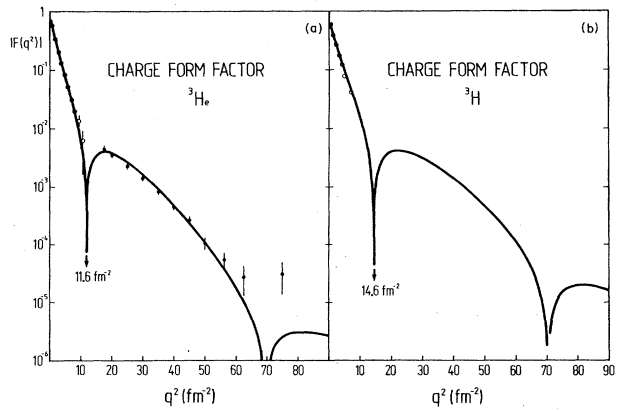

FIG. 3. Charge form factors of ^{3}He and ^{3}H. Data points are from Refs. 5, 6, and 8, and curves are the results of the model [Eqs. (14) and (17)] with parameters given in the Appendix.

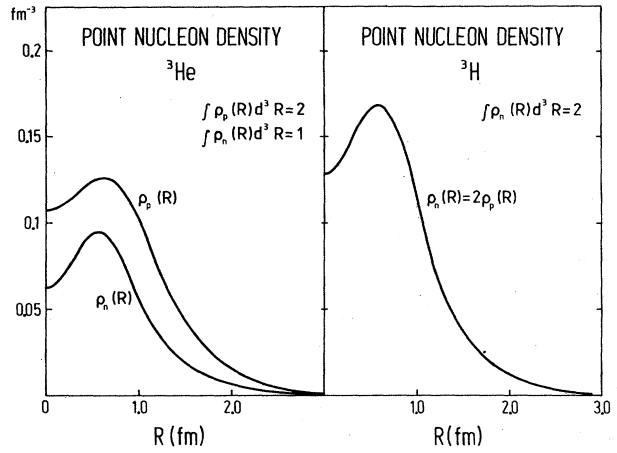

FIG. 4. Point-nucleon density in ^{3}He and ^{3}H corresponding to the body form factors [Eq. (17)]. Explicit expressions are given in the Appendix.

and the subsequent slow falloff. A second minimum is predicted at $q^2=70$ fm^{-2}, though this depends somewhat on the assumed behavior of the neutron charge form factor at large q^2. The parameters of this fit (see Appendix) now yield a prediction for the corresponding behavior of the triton charge form factor, shown in Fig. 3(b). The first minimum occurs at $q^2=14.6$ fm^{-2}. The subsequent maximum is at $q^2=22$ fm^{-2} and has almost the same height as the corresponding maximum in ^{3}He. A second minimum occurs at $q^2=70$ fm^{-2}. Current experiments will probe the triton form factor to about $q^2=25$ fm^{-2} (Ref. 9) and should be able to check the behavior shown in Fig. 3(b).

In Fig. 4, we show the effective point-nucleon densities $\rho_{n,p}(R)$ for ^{3}He and ^{3}H obtained from the Fourier transforms of Eq. (17). The explicit expressions are given in the Appendix. The depression at $R=0$ reflects the absence of matter at the center of the triangle correlation, and has been built into the parametrization of δF. With the densities normalized to $\int \rho(R)d^3R=1$, charge symmetry violation is reflected in $\rho_{p,n}(^3\mathrm{H})\neq\rho_{n,p}(^3\mathrm{He})$. Since the model assumes $\rho_p(^3\mathrm{H})=\rho_n(^3\mathrm{H})$, the difference $\rho_p(^3\mathrm{He})\neq\rho_n(^3\mathrm{He})$ reflects entirely the Coulomb distortion ($\eta_p\neq\eta$) of the triangle correlation.

V. COMMENTS AND CONCLUSIONS

We have suggested in this paper that the effects observed in $\pi^\pm$ elastic scattering from ^{3}H and ^{3}He can be understood in terms of a short-distance correlation of the three-nucleon system, whose distortion in going from ^{3}H to ^{3}He produces the charge-symmetry violation shown in Fig. 1. The amount of distortion may be judged from the difference between the parameters η^2, η_p^2, and η_n^2 which are in the ratio $\eta^2:\eta_p^2:\eta_n^2=0.33:0.45:0.27$. Correspondingly the radial distances shown in Fig. 2 are in the ratio $R_t:R_p:R_n=1:1.16:0.90$. We have taken the view that the origin of this distortion is the Coulomb repulsion of the two protons in ^{3}He, but the amount of distortion must clearly depend on the strong forces that are at work in this correlation. A test of the hypothesis lies in the behavior of the ratios r_1, r_2, and R for scattering in backward directions ($\theta>90°$). (This behavior may be tempered by multiple scattering corrections, but the qualitative trend shown in Fig. 1 should survive.)

We have argued that the same three-nucleon correlation is probed in electron scattering from these nuclei at high q^2. The pattern of dips and maxima observed in the charge form factor of ^{3}He is connected with the fine structure of this correlation. Once this structure is parametrized (as spelled out in the Appendix), the positions of the minima and maxima in ^{3}H are predictable in terms of the same distortion parameters η_p and η_n determined from pion scattering. A measurement of the triton charge form factor at large q^2 would thus serve as an important check of the internal consistency of the model.

Within the model, the different charge radii of ^{3}He and ^{3}H are attributed to the Coulomb repulsion of the two protons which causes the protons in ^{3}He to spread out spatially compared to the proton in ^{3}H. This effect is phenomenologically represented by the larger uncorrelated radius ($R_2>R_1$) of ^{3}He and by the distortion of the short-range correlation ($\eta_p>\eta$). As seen from Eq. (16), both of these effects contribute to the difference $\langle R^2\rangle^{^3\mathrm{He}}_{\mathrm{charge}}-\langle R^2\rangle^{^3\mathrm{H}}_{\mathrm{charge}}$. It should be noted, however, that a difference in the charge radii of ^{3}He and ^{3}H is not, *per se*, a charge-symmetry violating effect, since this symmetry is a statement about the matter form factors [Eq. (2)]. Even within a charge-symmetric framework, it is possible to imagine that the matter form factor associated with the like nucleons (protons in ^{3}He, neutrons in ^{3}H) differs from that associated with the unlike nucleon, because of the difference in the triplet and singlet two-nucleon interaction.[10] A weaker force between pp (and nn) compared to np can cause the protons in ^{3}He to spread out, independently of Coulomb repulsion effects. It is possible that the unequal radii $R_2>R_1$ required by our parametrization reflect, in part, a dynamical effect of this type. To the same extend, our assumption of a common distribution for p and n in ^{3}H is an approximation.

A remark may be made here on the magnetic form factors of ^{3}H and ^{3}He for which data are also available.[5,6] Within the model a statement about these quantities is possible if we make the crude assumption that the magnetic form factors are determined entirely by the spatial distribution of the odd nucleon, i.e.,

$$F^{^3\mathrm{H}}_{\mathrm{mag}}=F^{^3\mathrm{H}}_{\mathrm{p}}\ ,\quad F^{^3\mathrm{He}}_{\mathrm{mag}}=F^{^3\mathrm{He}}_{\mathrm{n}}\ . \tag{18}$$

Such an assumption would be valid, for instance, if the like nucleons were paired to spin zero and all orbital angular momenta were neglected. [Recall that in this limit, one obtains $\mu(^3\mathrm{He})=\mu_n=-1.91\ \mu_N$, $\mu(^3\mathrm{H})=\mu_p=2.79\ \mu_N$, to be compared with the experimental values -2.12 and $2.97\ \mu_N$, respectively.] Using the parameters (13) of the fit to the $\pi^\pm$ data, we obtain the magnetic radii

$$\langle R^2\rangle^{^3\mathrm{H}}_{\mathrm{mag}}=(1-\epsilon)R_1^2+6\epsilon\eta^2R_N^2+\langle r^2\rangle_{\mathrm{p,mag}}=(1.75\ \mathrm{fm})^2\ , \tag{19}$$

$$\langle R^2\rangle^{^3\mathrm{He}}_{\mathrm{mag}}=(1-\epsilon)R_2^2+6\epsilon\eta_n^2R_N^2+\langle r^2\rangle_{\mathrm{n,mag}}=(1.77\ \mathrm{fm})^2\ ,$$

where we have taken the magnetic radius of the proton and neutron to be $\langle r^2\rangle_{p,mag}=\langle r^2\rangle_{n,mag}=0.7$ fm^2. These numbers are to be compared with the measured values 1.70 ± 0.05 fm for ^{3}H,[6] and 1.74 ± 0.10 fm (Ref. 6) or 1.95 ± 0.11 fm (Ref. 5) for ^{3}He. Furthermore, within the same approximation, the high q^2 behavior of the magnetic form factors shows a dip at q^2 between 14 and 15 fm^{-2} in the case of ^{3}H, and at q^2 between 17 and 18 fm^{-2} for ^{3}He. The prediction for ^{3}He is remarkably close to the experimentally measured minimum at $q^2=18$ fm^{-2}.[11]

Finally, we have made a check of the accuracy of our parametrization of the body form factors of ^{3}H and ^{3}He by evaluating the following formula that has been proposed[12] for the ^{3}He-^{3}H binding energy difference:

$$\mathrm{BE}(^3\mathrm{He})-\mathrm{BE}(^3\mathrm{H})=\frac{e^2}{2\pi^2}\int_0^\infty dq[f_p^2(q^2)-f_n^2(q^2)][\tfrac{4}{3}F_n^{^3\mathrm{H}}(3q^2)-\tfrac{1}{3}F_p^{^3\mathrm{H}}(3q^2)]\ . \tag{20}$$

This formula is derived under the assumption of charge symmetric body factors [Eq. (2)], and the integral is dominated by the low q^2 region. We have verified that the charge symmetric limit of our form factors ($R_1=R_2$, $\eta_p=\eta=\eta_n$) gives the result 0.63 MeV, which coincides with the well-known result[12] obtained by direct evaluation using electron scattering data. (The discrepancy between this value and the actual binding energy difference of 0.76 MeV remains a problem, outside the purview of the present model.)

To conclude, the model for the spatial structure of the ^{3}H-^{3}He nuclei proposed in this paper can account for the unusual charge-symmetry violating effects observed in $\pi^\pm$ scattering, and is also compatible with the low q^2 electric and magnetic properties of this system. When adapted to the high q^2 structure of the ^{3}He charge form factor, it yields a prediction for the corresponding structure in ^{3}H. An approximate argument has been given for the magnetic form factors, which produces a dip in $F_{mag}^{^3\mathrm{He}}$ at the experimentally correct position. Interesting behavior of charge symmetry violation is predicted in $\pi^\pm$ scattering at large angles ($\theta>90°$). Several refinements to the model can be imagined (e.g., Fermi motion, multiple scattering, incomplete pairing of like nucleons to spin zero, different body form factors for p and n in ^{3}H, etc.). On a more fundamental level, one can ask if the geometrical features (e.g., the triangle correlation) discussed here can be derived from a dynamical model which includes three-body forces (ideas on this question may be found in Ref. 13). For the present, we look forward with great interest to new information from forthcoming experiments probing the structure of ^{3}He and ^{3}H with pion and electron beams.[14]

APPENDIX

The body form factors for ^{3}H and ^{3}He are parametrized as follows:

$$F_{p,n}^{^3\mathrm{H}}(q^2)=(1-\epsilon)e^{-R_1^2q^2/6}+\epsilon[e^{-\eta^2R_N^2q^2}+\delta F^{^3\mathrm{H}}(q^2)]\ ,$$
$$F_{p,n}^{^3\mathrm{He}}(q^2)=(1-\epsilon)e^{-R_2^2q^2/6}\epsilon[e^{-\eta_{p,n}^2R_N^2q^2}+\delta F_{p,n}^{^3\mathrm{He}}(q^2)]\ , \tag{A1}$$

where

$$\delta F^{^3\mathrm{H}}(q^2)=A\eta^2q^2\left[-e^{-\eta^2R_N^2q^2a}+\frac{\sin(\sqrt{3}\eta q\bar{R})}{\sqrt{3}\eta q\bar{R}}e^{-\eta^2R_N^2q^2b}\right],$$
$$\delta F_{p,n}^{^3\mathrm{He}}(q^2)=A\eta_{p,n}^2q^2\left[-e^{-\eta_{p,n}^2R_N^2q^2a}+\frac{\sin(\sqrt{3}\eta_{p,n}q\bar{R})}{\sqrt{3}\eta_{p,n}q\bar{R}}\times e^{-\eta_{p,n}^2R_N^2q^2b}\right]. \tag{A2}$$

The fits to the low q^2 data determine the parameters ϵ, η, η_p, η_n, R_1, and R_2 to be

$$\epsilon=0.27,\ R_1=1.67\text{ fm},\ R_2=1.74\text{ fm}$$
$$\eta^2=0.33,\ \eta_p^2=0.45,\ \eta_n^2=0.27\ . \tag{A3}$$

[The parameters η^2, η_p^2, and η_n^2 are related by Eq. (6)]. The additional parameters which appear in the correction terms δF control the high q^2 behavior of the form factors. These were adjusted to fit the charge form factor of ^{3}He, using Eqs. (14) and (15). The fit shown in Fig. 3(a) is obtained with the parameters

$$A=0.16\text{ fm}^2,\ \bar{R}=0.75\text{ fm},\ b=0.31,\ a=0.75\ . \tag{A4}$$

A constraint $a=b+\frac{1}{2}\bar{R}^2/R_N^2$ was imposed to ensure that the terms δF vanish as q^4 when $q^2\to0$, thus having very little influence in the low q^2 region.

The dips in $|F_{charge}^{^3\mathrm{H}}(q^2)|$ and $|F_{charge}^{^3\mathrm{He}}(q^2)|$ occur at the zeros of these form factors. The location of the first dip is determined by the cancellation of the oscillating terms proportional to $\sin(\sqrt{3}q\bar{R}\eta)$ or $\sin(\sqrt{3}q\bar{R}\eta_{p,n})$ and the remaining terms. The second dip in ^{3}H occurs essentially at the second zero of $\sin(\sqrt{3}q\bar{R}\eta)$, i.e., at $q^2=[2\pi/(\sqrt{3}\bar{R}\eta)]^2$. In the case of ^{3}He, the second minimum is intermediate between the second zero of $\sin(\sqrt{3}\eta_p\bar{R}q)$ and the second zero of $\sin(\sqrt{3}\eta_n\bar{R}q)$, i.e., at q^2 between $[2\pi/(\sqrt{3}\bar{R}\eta_p)]^2$ and $[2\pi/(\sqrt{3}\bar{R}\eta_n)]^2$.

The spatial density of nucleons $\rho_{p,n}(R)$ in ^{3}H and ^{3}He is given by the Fourier transforms of the body form factors, i.e.,

$$\rho_{p,n}^{^3\mathrm{H}}(R)=\int F_{p,n}^{^3\mathrm{H}}(q^2)e^{i\mathbf{q}\cdot\mathbf{R}}d^3q/(2\pi)^3\ ,$$
$$\rho_{p,n}^{^3\mathrm{He}}(R)=\int F_{p,n}^{^3\mathrm{He}}(q^2)e^{i\mathbf{q}\cdot\mathbf{R}}d^3q/(2\pi)^3\ . \tag{A5}$$

These are obtained from Eq. (A1) using the formulas

$$\int \frac{d^3q}{(2\pi)^3} e^{-i\mathbf{q}\cdot\mathbf{R}} e^{-Kq^2} = \frac{1}{8\pi^{3/2}} \frac{1}{K^{3/2}} e^{-R^2/4K} ,$$

$$\int \frac{d^3q}{(2\pi)^3} e^{-i\mathbf{q}\cdot\mathbf{R}} q^2 e^{-Kq^2} = \frac{1}{8\pi^{3/2}} \frac{1}{K^{5/2}} \left[\frac{3}{2} - \frac{R^2}{4K} \right] e^{-R^2/4K} ,$$

$$\int \frac{d^3q}{(2\pi)^3} e^{-i\mathbf{q}\cdot\mathbf{R}} q^2 e^{-Kq^2} \left[\frac{\sin qR_0}{qR_0} \right] = \frac{1}{8\pi^{3/2}} \frac{1}{2R_0R} \left\{ e^{-(R-R_0)^2/4K} \left[1 - \frac{(R-R_0)^2}{4K} \right] - e^{-(R+R_0)^2/4K} \left[1 + \frac{(R+R_0)^2}{4K} \right] \right\} . \tag{A6}$$

The densities defined by Eq. (A5) are normalized to $\int \rho_{p,n}(R) d^3R = 1$. Those plotted in Fig. 4 are normalized to the number of protons or neutrons in the relevant nucleus.

---

*Present address: Research Institute for Fundamental Physics, Kyoto, Japan.

[1]B. M. K. Nefkens *et al.*, Phys. Rev. Lett. **52**, 735 (1984).
[2]Y. E. Kim and A. Tubis, Annu. Rev. Nucl. Sci. **24**, 69 (1974); A. C. Phillips, Rep. Prog. Phys. **40**, 905 (1977).
[3]R. B. Wiringa *et al.*, Phys. Lett. **143B**, 273 (1984), and references therein.
[4]D. Robson, Nucl. Phys. **A308**, 381 (1978); Prog. Part. Nucl. **8**, 279 (1982).
[5]J. S. McCarthy, I. Sick, and R. R. Whitney, Phys. Rev. C **15**, 1396 (1977); I. Sick, *Lecture Notes in Physics, Vol. 87* (Springer, Berlin, 1978), p. 276.
[6]H. Collard *et al.*, Phys. Rev. **138**, B57 (1965).
[7]*Electron Scattering and Nuclear and Nucleon Structure,* edited by R. Hofstadter (Benjamin, New York, 1963); W. Bertozzi *et al.*, Phys. Lett. **41B**, 408 (1977).
[8]R. G. Arnold *et al.*, Phys. Rev. Lett. **40**, 1429 (1978).
[9]I. Sick, private communication.
[10]L. Schiff, Phys. Rev. **133**, B1153 (1963).
[11]J. M. Cavedon *et al.*, Phys. Rev. Lett. **49**, 986 (1982).
[12]J. L. Friar, Nucl. Phys. **A156**, 43 (1974); P. Sauer, *Lecture Notes in Physics, Vol. 86* (Springer, Berlin, 1978), p. 288.
[13]W. Glöckle and P. U. Sauer, Europhysics News, Vol. 15, No. 2, 1984, p. 1; S. Barshay, Phys. Lett. **100B**, 376 (1981); D. Robson, Ref. 4.
[14]R. Arnold, Stanford Linear Accelerator Center Report No. SLAC-PUB-3216, 1984; B. Nefkens and I. Sick, private communication.